Computers & Geosciences 85 (2015) 74–85

Contents lists available at ScienceDirect

Computers & Geosciences

journal homepage: www.elsevier.com/locate/cageo

A seed expanding cluster algorithm for deriving upwelling areas on sea surface temperature images

Susana Nascimento [a,b,*], Sérgio Casca [b], Boris Mirkin [c,d]

[a] Department of Computer Science, Faculdade de Ciências e Tecnologia, Universidade Nova de Lisboa, 2829-516 Caparica, Portugal
[b] NOVA Laboratory for Computer Science and Informatics (NOVA LINCS), Faculdade de Ciências e Tecnologia, Universidade Nova de Lisboa, 2819-516 Caparica, Portugal
[c] Department of Data Analysis and Machine Intelligence, National Research University Higher School of Economics, Moscow, Russian Federation
[d] Department of Computer Science, Birkbeck University of London, UK

ARTICLE INFO

Article history:
Received 2 October 2014
Received in revised form
4 March 2015
Accepted 8 June 2015
Available online 10 June 2015

Keywords:
Seeded region growing
Approximate clustering
Homogeneity criterion
SST images
Upwelling

ABSTRACT

In this paper a novel clustering algorithm is proposed as a version of the seeded region growing (SRG) approach for the automatic recognition of coastal upwelling from sea surface temperature (SST) images.

The new algorithm, one seed expanding cluster (SEC), takes advantage of the concept of approximate clustering due to Mirkin (1996, 2013) to derive a homogeneity criterion in the format of a product rather than the conventional difference between a pixel value and the mean of values over the region of interest. It involves a boundary-oriented pixel labeling so that the cluster growing is performed by expanding its boundary iteratively. The starting point is a cluster consisting of just one seed, the pixel with the coldest temperature. The baseline version of the SEC algorithm uses Otsu's thresholding method to fine-tune the homogeneity threshold. Unfortunately, this method does not always lead to a satisfactory solution. Therefore, we introduce a self-tuning version of the algorithm in which the homogeneity threshold is locally derived from the approximation criterion over a window around the pixel under consideration. The window serves as a boundary regularizer.

These two unsupervised versions of the algorithm have been applied to a set of 28 SST images of the western coast of mainland Portugal, and compared against a supervised version fine-tuned by maximizing the *F*-measure with respect to manually labeled ground-truth maps. The areas built by the unsupervised versions of the SEC algorithm are significantly coincident over the ground-truth regions in the cases at which the upwelling areas consist of a single continuous fragment of the SST map.

1. Introduction

The coastal ocean of Portugal is under the influence of northerly winds which are favorable to the occurrence of upwelling during the summer. This is a phenomenon that manifests at the surface by cold, less salty and nutrient-rich waters over the whole shelf, and by filaments of upwelled waters penetrating into the open ocean. Therefore, coastal upwelling is a phenomenon of ocean dynamics whose study is fundamental to the development of climate models and resulting applications relevant to fisheries, coastal monitoring and detection of pollutants. The identification and continuing monitoring of upwelling is thus a crucial part for the study of the dynamics of the oceans, which involves analyzing large volumes of data such as remote sensing images in the infrared range. The identification of upwelling is frequently analyzed with sea surface temperature (SST) images because of the temperature contrast between the cold7 upwelling waters and the warmer near-shore oceanic waters. These SST maps are typically obtained with the thermal infrared channels of the advanced very high resolution radiometer (AVHRR) sensor on board NOAA-n satellite series.

Several approaches have been proposed for automatic upwelling detection, each involving rather complex computations to achieve satisfactory segmentation results. For example, the works by Kriebel et al. (1998), Arriaza et al. (2003) and Chaudhari et al. (2008), using artificial neural networks, require the extraction of various morphological features followed by a region building using an iterative thresholding process. Marcello et al. (2005) used an extensive comparison of automatic thresholding techniques followed by a combination of watershed transform and region growing approaches. Nieto et al. (2012) developed an upwelling front detection system based on edge detection using a combination of multiple windows followed by a thorough process of

* Corresponding author. Fax: +351 21 294 8541.
E-mail address: snt@fct.unl.pt (S. Nascimento).

http://dx.doi.org/10.1016/j.cageo.2015.06.002
0098-3004/

recovering missing segments.

In our previous work (Nascimento and Franco, 2009; Nascimento et al., 2012), we characterized and automated the process of delineation of upwelling regions and boundaries using a fuzzy clustering method supplemented with what is referred to as anomalous cluster initialization process. Our system, FuzzyUPWELL, has proven to work rather reliably on the available collections of oceanographic images. Yet the system has an evident empiric flavor. It operates over the temperature data only, and uses no geographic information. Also, the system needs some expert driven knowledge to fine-tune thresholds which is not always easy to operationalize.

In this paper, we tackle the problem of determination of upwelling regions by using pixels and their spatial arrangement on temperature maps using a model inspired on the development of the upwelling as a process of step-by-step adding pixels according to the similarity of their temperatures to the temperatures of those already in the region. To this end, we adopt and considerably modify the popular seeded region growing (SRG) method introduced by Adams and Bischof (1994) for region based segmentation (see also e.g. Mehnert and Jackway, 1997; Freixenet et al., 2002; Fan et al., 2005; Shih and Cheng, 2005; Verma et al., 2011). This method tries to grow a region whenever its interior is homogeneous according to a certain feature such as intensity, color or texture, called the *feature of interest* (FoI). The algorithm follows the strategy based on the growth of a region, starting from one or several 'seeds' and by adding similar neighboring pixels. The growth is controlled by using a homogeneity criterion so that the merging decision is generally taken based only on the contrast between the evaluated pixel and the region. However, it is not always easy to decide when this difference is small (or large) enough to make a reasonable decision (Freixenet et al., 2002).

The seeded region growing image segmentation approach has been widely used in various medical image applications like magnetic resonance image analysis and unsupervised image retrieval in clinical databases (Mancas et al., 2005; Whitney et al. (2006); Wu et al., 2009; Harikrishna-Rai and Gopalakrishnan-Nair, 2010; Zanaty, 2013). The approach has been also successfully applied in color image segmentation with applications in medical imaging, content-based image retrieval, and video (Fan et al., 2001; Shih and Cheng, 2005; Ugarriza et al., 2009; Verma et al., 2011), and yet in remote sensing image analysis (Wang et al., 2010; Byun et al., 2011; Zhang et al., 2013).

Main challenging issues that arise with SRG methods are as follows:

(i) How to select the initial seeds in practice, and how critical is the seed selection to getting a good segmentation?
(ii) How to choose the region homogeneity criterion and how to specify its threshold?
(iii) How to organize the pixel labeling procedure efficiently?

Most approaches to SRG involve homogeneity criteria in the format of difference of the feature of interest between that at the pixel to be labeled and the mean value at the region of interest (Adams and Bischof, 1994; Zhou et al., 2004; Fan et al., 2005; Shih and Cheng, 2005; Ibrahim et al., 2010; Verma et al., 2011). A weak point of these algorithms is the definition of the non-homogeneity threshold at which the pixels under consideration are considered as failing the homogeneity test and, therefore, cannot be added to the region. Such a definition is either expert driven or supervised in most of the currently available algorithms (Zhou et al., 2004; Fan et al., 2005; Mat-Isa et al., 2005; Shih and Cheng, 2005; Ibrahim et al., 2010; Verma et al., 2011). Another issue of the SRG methods is the pixel ordering for testing them on joining the growth region and labeling (Mehnert and Jackway, 1997). Many SRG algorithms grow the regions using a sequential list sorted according to the dissimilarity of unlabeled pixels to the growth region (Adams and Bischof, 1994; Grinias and Tziritas, 2001; Harikrishna-Rai and Gopalakrishnan-Nair, 2010; Verma et al., 2011). The disadvantage is that the segmentation results are very much sensitive to this order.

To meaningfully overcome these issues, we apply the concept of approximate cluster from Mirkin (1996, 2013) to the SRG framework. This approximation approach leads us to accept a mathematically equivalent, though somewhat unusual, homogeneity criterion, in the format of a product rather than the conventional difference between the pixel and the mean of the region of interest. Specifically, to segment an SST map, we first subtract the average temperature value from all the temperature values. After this, a pixel p under consideration is added to the cluster if and only if $c \times t(p) \geq \pi$ where c is the average temperature of the pixels already in the cluster, $t(p)$ the temperature of the pixel p, and π a threshold defined by the maximum difference between cold water pixels and the rest. This process is moderated via usage of the concept of window of a pre-specified size around the pixels under consideration: only those within the window are involved in the comparison processes. This provides for the spatial homogeneity and smoothness of the growing region. Indeed, only borderline pixels are subject to joining in because the windows around remote pixels just do not overlap the growing region. Therefore, there is no need in specifying the order of testing for labeling among pixels: all those borderline pixels can be considered and decided upon simultaneously. The process starts from a cluster consisting of just one pixel, the coldest one, according to the approximation clustering criterion. The preprocessed temperature of this pixel is negative with a relatively large absolute value. Since the temperature is a rather conservative characteristic and would not change sharply with respect to space, there must be a bulk of pixels within the window centered at the starting point that will have similarly cold temperatures so that the products of those by the preprocessed temperature at the seed have large positive values and thus have to join in the growing region. This shows that our region growing process initializes with a fragment of the coldest pixels, which is rather robust. Using the window as a constraint brings forth another desirable property. The growing region in our process normally would cover a continuous fragment of the ocean. To warrant this, we tried an additional homogeneity condition: the density of the cluster being built should be greater than or equal to a threshold α. The density is defined locally as the fraction of pixels belonging to the cluster in the window surrounding the pixel under consideration. Yet this proved unnecessary in our experimental computations: the spatial continuity of the region has been warranted by the step-by-step procedure of the growing region to reach out of the boundary in all directions. The proposed method, one seed expanding cluster (SEC), holds out of the issue of dependence on the pixel sorting order. Moreover, the simultaneous borderline labeling considerably speeds up the SRG procedure.

To specify the similarity threshold to judge whether the pixel under consideration should be added to the growing region or not, we take Otsu's (1979) thresholding method. This method fine-tunes the similarity threshold by finding the maximum inter-class variance that splits between warm and cold waters. This defines what we refer to as the baseline version of the SEC algorithm. Also, we introduce a self-tuning version of the algorithm, SelfT-SEC, at which the homogeneity threshold parameter is derived from the cluster approximation criterion.

These two unsupervised versions of the SEC algorithm have been applied to a set of 28 SST images of the western coast of mainland Portugal, and compared against a supervised version fine-tuned by maximizing the F-measure with respect to ground-truth maps annotated by expert oceanographers.

The rest of the paper is organized as follows. Section 2 describes the original SRG method. In Section 3 we describe the new seed expanding cluster algorithm, derive its optimal homogeneity

criterion, and present an extension of the algorithm to its self-tuning version. Section 4 presents the imagery data of SST's and discusses the results of the experimental study comparing two unsupervised thresholding versions of the SEC algorithm against the supervised thresholding version. Conclusions and future work are in Section 5.

2. The seeded region growing method

The original seeded region growing (SRG) method by Adams and Bischof (1994) can be summarized as follows.

Choose K initial sets of seeds $A_1, A_2, \ldots, A_K$, each one being a set of image neighboring pixels taking the feature of interest for analysis. From the initial seeds grow homogeneous regions $C_1, C_2, \ldots, C_K$ by merging the additional pixels one by one according to a similarity criterion, with the seeds being replaced by centroids of the homogeneous regions. The pixels belonging to the same region C_k, $(k = 1, 2, \ldots, K)$ are labeled by k, and pixels in different regions are labeled differently. The result of the algorithm is a segmentation map $(C_1, C_2, \ldots, C_K)$ with $A_k \subseteq C_k$ and $C_k \cap C_l = \varnothing$, $(k \neq l)$, where $\bigcup_{k=1}^{K} C_k = \Omega$ covers the whole image.

At each step of the algorithm, let B be the set of all yet unallocated pixels (i,j) which are adjacent to at least one of the already labeled regions C_k:

$$B = \left\{ (i,j) \notin \bigcup_{k=1}^{K} C_k | N(i,j) \cap \bigcup_{k=1}^{K} C_k \neq \varnothing \right\} \tag{1}$$

with $N(i,j)$ the set of immediate neighbors of the pixel.[1]

Then one pixel of the borderline set B, that one with the lowest dissimilarity to the K regions, is removed from B and labeled. The algorithm stops when the borderline set B is empty. The labeling process proceeds as follows. For a pixel $(i,j) \in B$, if $N(i,j)$ intersects only one currently labeled region C_k, then, pixel (i,j) will be labeled as $\ell(i,j) = k$ $(k \in \{1, 2, \ldots, K\})$. The similarity criterion $\delta((i,j), C_k)$ is defined as the difference between the pixel $(i,j) \in B$ and its adjacent labeled region C_k, that is,

$$\delta((i,j), C_k) = |g(i,j) - g(\bar{i}_k, \bar{j}_k)| \tag{2}$$

where $g(i,j)$ indicates the value of the feature of interest at the test pixel (i,j), and $g(\bar{i}_k, \bar{j}_k)$ represents the average value for all the pixels belonging to region C_k, with $(\bar{i}_k, \bar{j}_k)$ the centroid point of C_k.

If $N(i,j)$ intersects two or more regions C_k, then (i,j) is assigned to the region k^* for which $\delta((i,j), C_{k^*})$ is minimum over all neighboring regions C_k, $\ell(i,j) = k^*$.

That means one takes among the points in B that one satisfying the relation

$$(\hat{i}, \hat{j}) = \text{argmin}_{(i,j)\in B}\{\delta((i,j), C_{\ell(i,j)})\} \tag{3}$$

and append $(\hat{i}, \hat{j})$ to $C_{\ell(i,j)}$.

The definitions (2) and (3) guarantee that the final segmentation corresponds to regions as homogeneous as possible subject to a connectivity constraint.

3. One seed expanding cluster algorithm

3.1. The baseline algorithm

Let $T(R, L)$ be a sea surface temperature (SST) map, where R is the set of rows and L the set of columns, and elements of $R \times L$ are pixels. The process starts by centering the temperature, that is, by subtraction of the average temperature $t^* = mean(T(R, L))$ of the temperature map T from the temperature values at all pixels in $R \times L$. Let the centered values be denoted as $t(i,j)$, $(i,j) \in R \times L$. The algorithm finds a cluster $C \subseteq R \times L$ in the format of a binary map $Z(R, L)$ with elements z_{ij} defined as $z_{ij} = 1$ if $(i,j) \in C$ and $z_{ij} = 0$, otherwise. The algorithm involves a window system W where $W(i,j)$ is rectangular window of a prespecified size centered at pixel (i,j). Based on our experiments we take 7 (pixels) as the window side so that a window is a square of the size 7×7.

The algorithm starts by selecting a seed pixel, $o = (i_o, j_o)$, as the pixel with the lowest temperature value (if several pixels satisfy this condition, then o is chosen randomly among them). The cluster C is initialized as the seed $o = (i_o, j_o)$ together with pixels within the window $W(i_o, j_o)$ satisfying the similarity condition

$$c \times t(i,j) \geq \pi, \tag{4}$$

where c is the reference temperature taken at the start as the temperature of the seed pixel o, and π, a similarity threshold.

Once cluster C is initialized, its *cluster boundary set* F is defined as the set of such unlabeled pixels (i.e. those not assigned to the cluster), that their 8-neighborhood intersects the cluster. This means that boundary pixels are adjacent to the cluster with respect to their 8- neighborhood. Therefore,

$$F = \{(i',j') \notin C | N(i',j') \cap C \neq \varnothing\} \tag{5}$$

with $N(i',j')$ being the 8-neighborhood of the pixel.

Then, the algorithm proceeds iteratively expanding the cluster C step by step by dilatating its boundary F until it is empty. For each boundary pixel (i',j') in F we define the boundary expand region as the subset of pixels (i,j) of C that intersect the exploring window centered at pixel (i',j'), that is, $(i,j) \in W(i',j') \cap C$ and define c^* as the average temperature of those pixels.

The homogeneity criterion of the algorithm is defined by two conditions: (i) the temperature similarity condition in (6) and (ii) a density condition in (7). The similarity condition (6) involves the reference temperature c^* equal to the mean temperature of the window pixels within the expanding region defined as $c^* = mean(T(W(i',j') \cap C))$:

$$c^* \times t(i',j') \geq \pi \tag{6}$$

We define the density of points at a boundary pixel (i',j') as the number of pixels of cluster C falling within the exploring window $W(i',j')$ related to the total number of pixels within $W(i',j')$. The density of cluster points should be higher than a certain threshold α. The density condition is thus defined as

$$\frac{|W(i',j') \cap C|}{|W(i',j')|} \geq \alpha. \tag{7}$$

This condition, basically, serves as a tool to keep the cluster being built of a more or less smooth shape, without getting thin irregular fragments.

If both homogeneity conditions (6) and (7) hold, then the boundary pixel (i',j') is allocated to an auxiliary cluster C' and consequently labeled, and the corresponding boundary pixels $N(i',j')$ are merged to the auxiliary boundary set F' (both C' and F' are initialized as empty sets). The process continues until all boundary pixels of F have been treated. At the end, the new labeled pixels in C' are merged with C and the corresponding boundary set F is updated with the auxiliary boundary set F'. The iterative process of expanding the boundary pixels of the cluster stops when the boundary set F is empty, that is, when no more unlabeled pixels satisfy the homogeneity conditions (6) and (7).

It is important to stress that this process of treating all frontline pixels of the cluster before updating the cluster and the

[1] A neighborhood of 8-connectivity is typically used.

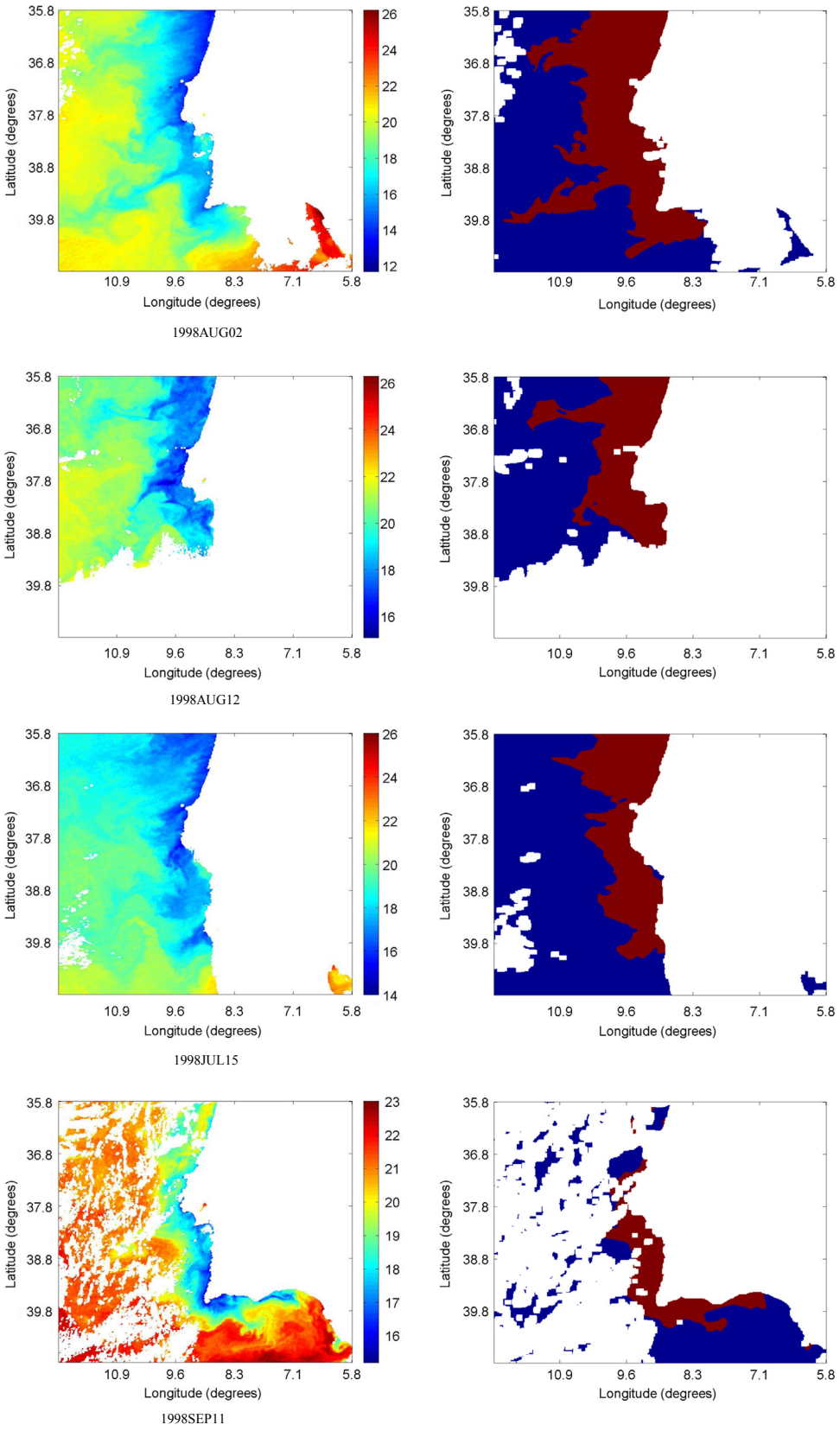

Fig. 1. Four SST images of Portugal showing different upwelling situations (left column) and corresponding binary ground-truth maps (right column).

corresponding new boundary set, guarantees that the cluster expansion does not depend on the order of selection of the boundary pixels to be treated. Moreover, the process of density and similarity conditions testing and labeling of the boundary pixels can be performed in parallel. This algorithm, designated as seed expanding cluster (SEC) algorithm, can be described by the following

Table 1
Similarity threshold values and segmentation evaluation scores when applying the SEC algorithm with supervised thresholding on the SST images of Portugal, organized in three groups: strong gradient, weak gradient, and noisy.

SST image	Similarity thresh. π	Precision	Recall	F-measure
Good				
1998-08-01	0.03	0.987	0.980	0.984
1998-07-28	0.6	0.979	0.984	0.981
1998-07-18	0.08	0.975	0.981	0.978
1998-08-02	0.01	0.990	0.965	0.977
1998-08-12	0.01	0.990	0.956	0.973
1998-08-21	0.8	0.964	0.977	0.971
1998-06-28	0.5	0.962	0.974	0.968
1998-07-03	0.55	0.918	0.971	0.944
1998-07-24	0.09	0.892	0.998	0.942
1998-08-30	0.09	0.942	0.937	0.940
1998-08-19	0.09	0.909	0.970	0.939
1998-08-05	0.5	0.994	0.848	0.915
1998-09-15	0.09	0.905	0.918	0.912
1998-09-05	0.5	0.988	0.844	0.910
1998-07-21	0.08	0.827	0.979	0.897
Weak grad.				
1998-09-08	0.70	0.984	0.967	0.976
1998-07-11	0.95	0.978	0.966	0.972
1998-06-25	0.65	0.968	0.971	0.969
1998-06-14	0.70	0.955	0.967	0.961
1998-06-23	0.60	0.949	0.953	0.951
1998-06-18	0.50	0.997	0.809	0.893
1998-07-15	0.65	0.976	0.800	0.879
1998-08-23	1.30	0.957	0.749	0.841
1998-09-24	1.05	0.809	0.532	0.642
Noisy				
1998-09-11	0.80	0.878	0.945	0.910
1998-09-30	0.09	0.718	0.995	0.834
1998-07-07	0.50	0.919	0.660	0.768
1998-08-10	0.04	0.570	0.815	0.670

computational scheme:

Input $T(R, L)$– temperature map, where R is the set of rows and L the set of columns;
w- side of the exploring window W
π- threshold of (temperature) similarity
α- threshold of cluster density
Output One cluster C in the format of a binary map $Z(R, L)$ over the same sets R and L with elements z_{ij} defined as: $z_{ij} = 1$ if $(i, j) \in C$ and $z_{ij} = 0$ if $(i, j) \notin C$.

Step 1 **Pre-processing:** Subtract the average temperature $t^* = mean(T(R, L))$ from the original temperature value of each pixel (i,j) of temperature map T. Let $t(i, j)$ be the temperature values after subtraction.

Step 2 **Cluster Initialization:** A seed pixel $o = (i_0, j_0)$ is taken as that with the minimum temperature value c.
Set cluster $C = \{(i_0, j_0)\}$.
Take the exploring window W centered at seed pixel o. Each pixel (i,j) within $W(i_0, j_0)$ is labeled as belonging into cluster C iff the similarity criterion holds:

$$c \times t(i, j) \geq \pi \tag{8}$$

Step 3 **Set Cluster Boundary:** Define the set F of boundary pixels of C as the unlabeled pixels (i', j') lying within map $R \times L$ that are adjacent to C, that is,

$$F = \{(i', j') \notin C | N(i', j') \cap C \neq \varnothing\} \tag{9}$$

with $N(i', j')$ the 8-neighborhood of the pixel.

Step 4 **Expansion**: **While** boundary set F is not empty
Step 4.1 Set $C' = \varnothing$; $F' = \varnothing$;
Step 4.2 **For** each boundary pixel $(i', j') \in F$
Step 4.2.1 Consider the *boundary expand region* as $W(i', j') \cap C$; define c^* as: $c^* = mean(T(W(i', j') \cap C))$
Step 4.2.2 **If** both the *similarity* and *density* conditions hold:

$$c^* \times t(i', j') \geq \pi \tag{10}$$

$$\frac{|W(i', j') \cap C|}{|W(i', j')|} \geq \alpha \tag{11}$$

then the frontline pixel is merged with the cluster and the boundary set F is updated with the 8-neighbors pixels of (i', j') disjoint from C:

$$C' = C' \cup \{(i', j')\}; F' = F' \cup N(i', j') - C \tag{12}$$

Step 4.3 **Update** C **and** F**:** $C = C \cup C'$; $F = F \cup F' - \{(i', j')\}$

3.2. Derivation of the similarity criterion and self-tuned threshold value

The idea is to find such a subset $C \subseteq R \times L$ that its binary matrix $z = (z_{ij})$, where $z_{ij} = 1$ if $(i, j) \in C$ and $z_{ij} = 0$ otherwise, approximates a given temperature map matrix $T(R, L)$ as close as possible. To accommodate for the difference in the unit of measurement of the similarity as well as for its zero point, matrix z should be also supplied with (adjustable) scale shift and rescaling coefficients, say λ and μ. That would mean that the approximation is sought in the set of all binary $\lambda + \mu/\mu$ matrices $\lambda z + \mu$ with $\lambda > 0$. Unfortunately, such an approximation, at least when follows the least squares approach, would have little value as a tool for producing a cluster, because the optimal values for λ and μ would not separate the optimal C from the rest. Therefore, following Mirkin (1996, 2013), only one parameter λ, the change of the unit of measurement, is utilized here. The issue of setting a similarity zero point is moved then out of the modeling stage to the data pre-processing stage. This should explain the subtraction of the average temperature before doing data analysis as the setting of a proper similarity zero point so that the structure is analyzed against a backdrop of the mean.

Then the approximation model can be stated as

$$t_{ij} = \lambda z_{ij} + e_{ij} \tag{13}$$

where t_{ij} are the preprocessed temperature values, $Z = (z_{ij})$ is the unknown cluster membership matrix and λ is the rescaling factor value, also referred to as the cluster intensity value. The items e_{ij} represent unspecified errors of the model, that should be made as small as possible. To fit the model (13), only the least squares criterion $\Phi^2 = \sum_{i \in R} \sum_{j \in L} e_{ij}^2 = \sum_{i \in R} \sum_{j \in L} (t_{ij} - \lambda z_{ij})^2$ is considered here.

First of all, note that at any given C, that is, matrix $Z = (z_{ij})$, the optimal value of λ is determined as the average temperature t_{ij} over all the within-C pixels $(i, j) \in C$. This easily follows from the first-order optimality condition for criterion Φ^2.

Although more or less conventional mathematically, the criterion Φ^2 bears somewhat unusual meaning substantively. Indeed, any $z_{ij} = 0$ contributes t_{ij}^2 to Φ^2 independently of the λ value. Therefore, $z_{ij} = 0$ should correspond to those pixels whose preprocessed temperatures $t(i, j)$ are zero or near zero. In contrast, pixels of maximum or almost maximum absolute values of the

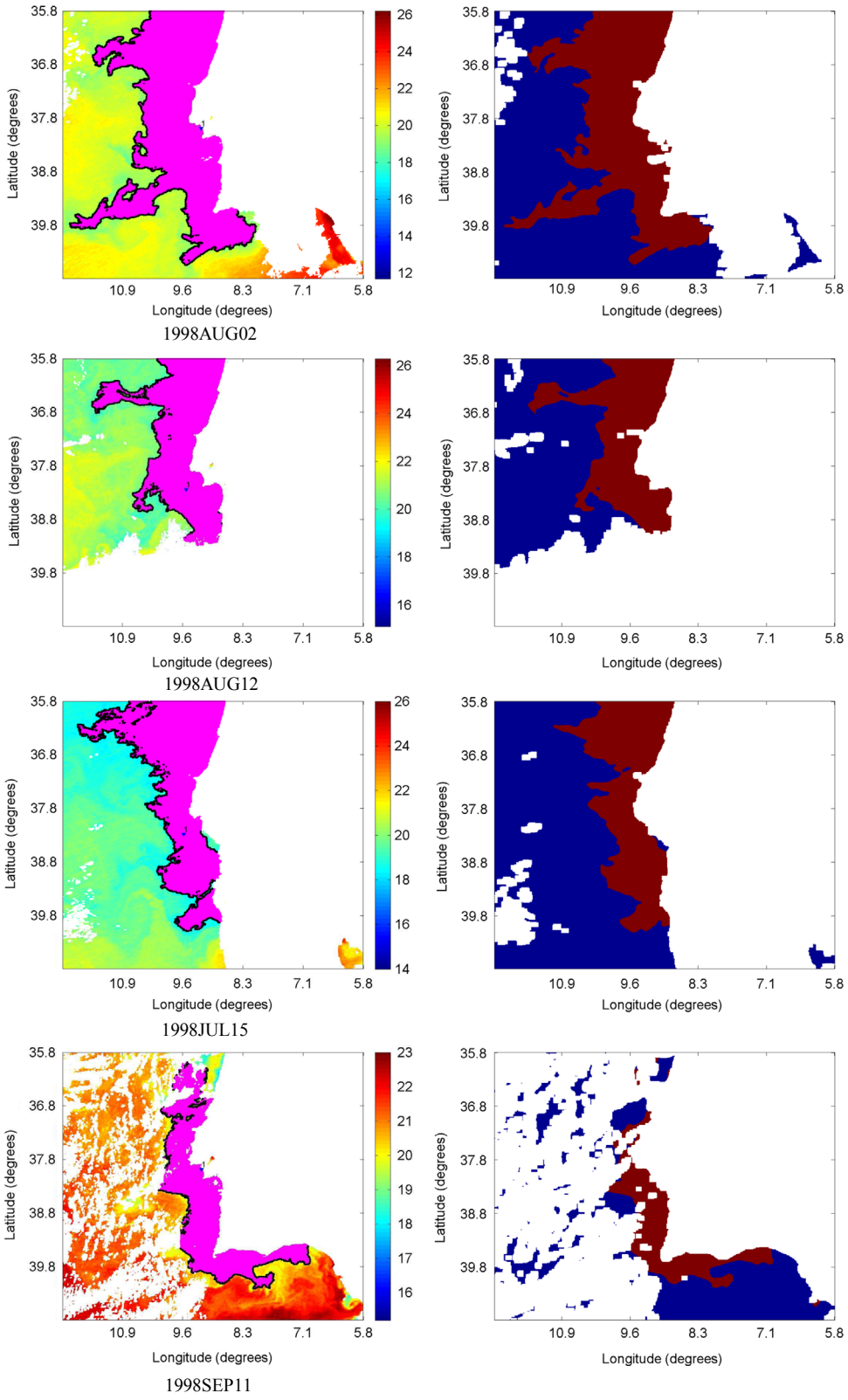

Fig. 2. Upwelling area retrieved by the SEC algorithm with supervised thresholding on SST images of Portugal (left column) and binary ground-truth maps of the images (right column).

temperature should be assigned with $z_{ij} = 1$. However, those must be either warmest or coldest pixels because any mix of them would make the optimal λ close to zero, thus keeping the Φ^2 value out of its minimum zone. The case is resolved based on our substantive knowledge: the upwelling areas comprise coldest waters. Therefore, cluster C should comprise negative temperature pixels as far from zero as possible. This justifies taking the coldest pixel as the starting point in SEC. Also, usefulness of initially subtracting the mean temperature with this approach manifests

Table 2
Similarity threshold values and segmentation evaluation scores when applying the SEC algorithm with Otsu's thresholding on the SST images of Portugal, organized in three groups: strong gradient, weak gradient, and noisy.

SST image	Similarity thresh. π	Precision	Recall	F-measure
Good				
1998-07-28	0.702	0.988	0.966	0.977
1998-08-19	0.475	0.990	0.888	0.936
1998-08-02	0.226	1.000	0.873	0.932
1998-06-28	0.265	0.855	0.999	0.921
1998-08-05	0.407	0.990	0.861	0.921
1998-09-15	0.049	0.885	0.935	0.909
1998-08-30	0.597	0.978	0.845	0.907
1998-08-12	0.325	1.000	0.817	0.899
1998-08-21	1.386	0.998	0.813	0.896
1998-07-24	0.698	1.000	0.770	0.870
1998-07-03	0.127	0.717	1.000	0.835
1998-07-21	0.939	0.953	0.720	0.821
1998-08-01	1.418	1.000	0.689	0.816
1998-09-05	0.072	0.590	0.906	0.715
1998-07-18	0.881	1.000	0.496	0.663
Weak grad.				
1998-06-18	0.479	0.996	0.820	0.900
1998-07-11	0.533	0.761	0.999	0.864
1998-07-15	0.911	0.997	0.746	0.853
1998-08-23	1.017	0.916	0.767	0.835
1998-09-08	0.088	0.705	1.000	0.827
1998-06-23	0.018	0.608	0.988	0.753
1998-06-25	0.064	0.542	1.000	0.703
1998-06-14	0.026	0.398	1.000	0.569
1998-09-24	0.077	0.390	0.667	0.492
Noisy				
1998-09-11	0.068	0.721	0.992	0.835
1998-09-30	0.060	0.695	0.996	0.819
1998-08-10	0.020	0.565	0.822	0.669
1998-07-07	1.000	0.992	0.356	0.524

itself once more.

Another observation comes from the expression for the criterion Φ^2 found by 'opening' parentheses in it. Specifically, since $z_{ij}^2 = z_{ij}$ because z_{ij} accepts only 0 and 1 values, the least squares criterion can be reformulated as

$$\Phi^2(C, \lambda) = \sum_{i\in R}\sum_{j\in L}(t_{ij} - \lambda z_{ij})^2 = \sum_{i\in R}\sum_{j\in L} t_{ij}^2 - 2\lambda \sum_{i\in R}\sum_{j\in L}(t_{ij} - \lambda/2)z_{ij} \quad (14)$$

As $\sum_{i\in R}\sum_{j\in L} t_{ij}^2$ is constant, at $\lambda > 0$, minimizing (14) is equivalent to maximizing the scoring function

$$f(C, \lambda) = \sum_{i\in R}\sum_{j\in L}\lambda(t_{ij} - \lambda/2)z_{ij} = \sum_{i,j\in C}\lambda(t_{ij} - \lambda/2). \quad (15)$$

Therefore, to maximize (15), pixels (i,j) at which $\lambda t_{ij} - \pi > 0$ where $\pi = \lambda^2/2$ should be added to C, whereas those at which $\lambda t_{ij} - \pi < 0$, should not. Since the optimal λ is the average temperature within C, this not only justifies our similarity criterion in (6) but also suggests that a self-tuned value of threshold π in (4) and (6) should be $\pi = \lambda^2/2$.

Therefore, in the follow-up we take the self-tuned value for the similarity threshold as half the squared average temperature over the cluster C.

A more or less smooth shape of the growing region is warranted by the averaging nature of the similarity criterion and by involving windows around all pixels under consideration. This structure of the clustering process allows us to abandon the density condition (7) in the self-tuning version of SEC algorithm.

3.3. Self-tuning version of the SEC algorithm

The SEC algorithm had been extended in order to automatically take into account the similarity threshold π according to the derivations in the previous section. In contrast to the baseline SEC algorithm, the threshold π in this version is not constant but changes depending on changes of C fragments falling in the windows $W(i, j)$.

This version of SEC in general follows the outline above except for the step of expanding the cluster (step 4.2.2 of the algorithm). That is altered in two points:

(i) the similarity threshold π in condition (6) is specified as $(mean(T(W(i', j') \cap C)))^2/2$;
(ii) the density condition (7) is abolished.

This makes a version of the algorithm SEC, designated as self-tuning seed expanding cluster algorithm, or ST-SEC for short. ST-SEC runs exactly as the SEC, up to the two adjustments, (i) and (ii) above.

4. Experimental study

4.1. Imagery data

A group of 28 AVHRR sea surface temperature (SST) images obtained during the period of June 1998–September 1998 are used in this study. A high resolution color scale (192 levels) was applied to each SST image in order to have the best distribution of color levels over the SST range in each individual image.

Each SST image, T, is represented by a 500×500 pixels map, with each sea pixel assigned with the temperature in degrees Celsius. The continuous white region on the right side of each SST image corresponds to land, whereas white pixels in the ocean part correspond to missing values during the satellite transmission, typically due to cloud cover. Each SST image is named according to the date of acquisition.

Fig. 1 (left column) shows four representative SST images selected from the benchmark data sample of Portugal, illustrating the variability of upwelling situations. Specifically: (i) SST images with a well-characterized upwelling situation in terms of fairly sharp boundaries between cold and warm surface waters measured by relatively contrasting thermal gradients and continuity along the coast (two topmost images); (ii) SST images showing distinct upwelling situations related to thermal transition zones offshore from the North toward the South and with smooth transition zones between upwelling regions; (iii) noisy SST images with clouds, where information to define the upwelling front lacks (fourth-line image). Each SST image has assigned a binary ground-truth map, manually constructed by expert oceanographers, with 1/0 labels corresponding to 'upwelling/non-upwelling' designations. Fig. 1 (right column) shows the corresponding ground-truth maps of the SST images on top.

4.2. Settings of the experiments

In this study we analyze the effectiveness of the SEC algorithm, both the baseline and the self-tuning versions, on segmenting SST images to automatically identify the upwelling area.

There is no generally accepted methodology for evaluating segmentation algorithms (Pal and Pal, 1993; Muñoz et al., 2003). We consider a supervised evaluation approach, also known as *empirical discrepancy* method, to analyze segmentation results by comparing them with corresponding manually segmented reference images, the ground-truths. The degree of similarity between the human and machine segmented images determines the quality of the segmentation. One benefit of supervised methods of evaluation over unsupervised ones is that direct comparison

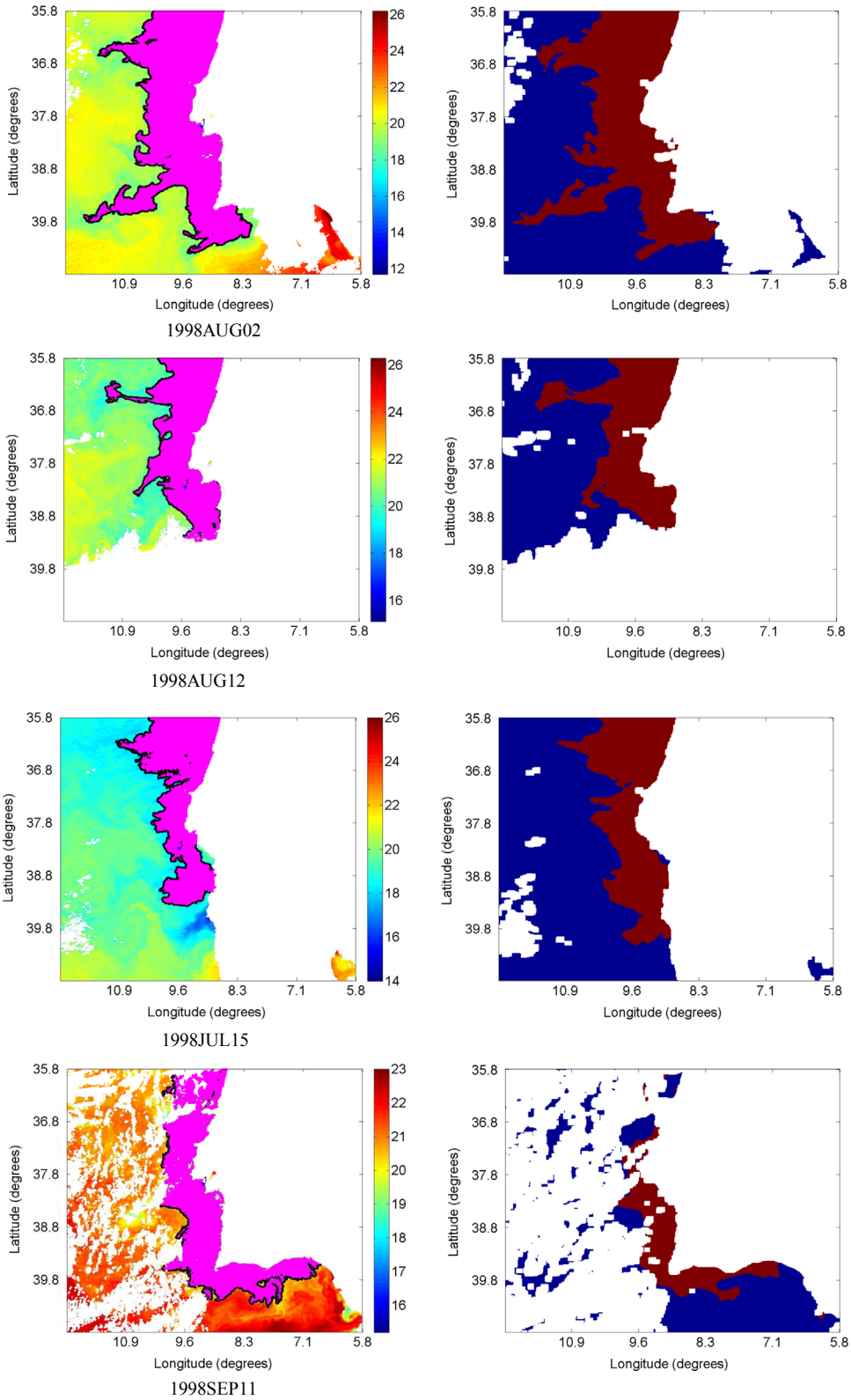

Fig. 3. Upwelling area retrieved by the SEC algorithm with Otsu's thresholding on SST images of Portugal (left column) and binary ground-truth maps of the images (right column).

between a segmented image and a reference image provides a finer resolution of evaluation and, as such, discrepancy methods are commonly used for an objective evaluation (Zhang et al., 2008).

To compare the performance of various results of seed region growing algorithms, typical measures commonly applied include precision, recall and the corresponding harmonic mean, the *F*-measure (Van Rijsbergen, 1979). Precision is the proportion of the predicted positive cases that are correctly real positives, while recall, or true positive rate, is the proportion of true positive cases

Table 3
Segmentation evaluation scores when applying the self-tuning version of the SEC algorithm on the SST images of Portugal, organized in three groups: strong gradient, weak gradient, and noisy.

SST image	Precision	Recall	*F*-measure
Good			
1998-08-01	0.990	0.957	0.974
1998-08-02	0.997	0.919	0.956
1998-07-18	0.930	0.980	0.955
1998-08-12	0.997	0.893	0.942
1998-08-30	0.946	0.925	0.935
1998-08-19	0.837	0.970	0.898
1998-07-28	0.813	0.999	0.896
1998-07-24	0.812	0.993	0.893
1998-09-15	0.863	0.920	0.891
1998-07-21	0.809	0.978	0.885
1998-08-05	0.848	0.876	0.862
1998-06-28	0.658	0.997	0.793
1998-07-03	0.655	0.997	0.790
1998-08-21	0.560	0.997	0.717
1998-09-05	0.569	0.957	0.713
Weak grad.			
1998-06-23	0.656	0.985	0.788
1998-07-15	0.645	0.991	0.781
1998-08-23	0.586	0.962	0.729
1998-09-08	0.533	0.997	0.695
1998-06-25	0.518	0.999	0.682
1998-06-14	0.479	0.997	0.647
1998-07-11	0.457	1.000	0.627
1998-06-18	0.422	0.980	0.590
1998-09-24	0.391	0.654	0.490
Noisy			
1998-09-11	0.728	0.987	0.838
1998-09-30	0.707	0.987	0.824
1998-07-07	0.686	0.692	0.689
1998-08-10	0.522	0.662	0.584

that are correctly identified. In other words, precision corresponds to the probability that the detection is valid, and recall is the probability that the ground truth is detected.

On running the baseline version of SEC algorithm we need a strategy to fine-tune the density and similarity thresholds, α and π. Preliminary experiments allow us to fix the density threshold at a constant value. In the experiments described in this study α had been fixed as the inverse of the size of window W, that is, $\alpha = 1/49$. To fine-tune the similarity threshold π, two different approaches have been considered: a supervised approach and an unsupervised one. In the supervised case, taking advantage of the ground-truth map, the threshold π is fixed as the one that maximizes the *F*-measure, by running the SEC algorithm with π ranging between $[0.01, 1.5]$ with an incremental step of 0.01. The first unsupervised approach is, Otsu's (1979) thresholding method, arguably the most popular thresholding method in the literature (Sezgin and Sankur, 2004). In this case, the optimum threshold value is fixed as the one presenting the minimum intra-class variance (i.e. the maximum between-class variance) when dichotomizing the pixels of the SST image in a bimodal histogram. Otsu's method is summarized in Appendix. Finally, we analyze the performance of the self-tuning thresholding version of the algorithm and make a comparative analysis of both unsupervised versions of thresholding against the supervised one.

4.3. Main results and discussion

Table 1 presents, for each SST image organized in the three groups: good, weak gradients, and noisy, the similarity threshold value obtained by maximizing the *F*-measure. For each group of images the results are presented in the descending order of *F*-measure values. The precision and recall values are also presented.

These results show that the segmentations are rather good, with 93% of *F*-scores ranging between 0.768 and 0.985. To illustrate the quality of the segmentation results, Fig. 2 (left column) presents the segmentations obtained by the SEC algorithm with the supervised fine-tuning for the images shown in Fig. 1. By comparing these results with the corresponding ground-truth maps of the images (right column), we can observe a real good matching that is reflected in the recall values close to 1.0.

The exceptions (with *F*-measure less than 0.7) occur for the images of '1998-08-10' and of '1998-09-24', the first with a low precision and high recall and the second with a high precision and low recall, and consequent relatively low *F*-measures. The first type of results corresponds to over-segmentation with 'explosion' in the North region covering a fraction of offshore area of cold temperatures. The second type of results corresponds to a coarse segmentation, meaning that the original image contains discontinuous upwelling areas, whereas the computation produces just one sub-region, thus leading to a low true positive rate.

The results of applying Otsu's thresholding version of the SEC algorithm are in Table 2. In this case 82% of segmentations present high *F*-measures ranging between 0.70 and 0.977. Fig. 3 (left column) illustrates the segmentation results of our algorithm with Otsu's thresholding. The results are very much coincident with the corresponding ground-truth maps displayed on the right.

Only five images present low *F*-measures corresponding to either small recall or precision values. In fact, the results with low recall values ($\leq$0.6) correspond to coarse segmentations due to the discontinuity of the upwelling areas. On the contrary, the segmentations with low precision ($\leq$0.6) correspond to over-segmented results, where the obtained cluster containing the total original upwelling area, expanding offshore, mainly in the cold waters of the North region. This type of unsuccessful results are typically associated with images at which the upwelling areas correspond to relatively small percentage of the SST image. This result is justified by the fact that this method is biased toward the components with larger class variance, tending to dichotomize an image into the object and background of similar sizes (Hou et al., 2006).

On analyzing segmentations obtained by the self-tuning threshold version of the algorithm we obtained very good results in 75% of the cases as shown by the evaluation scores presented in Table 3 taking the *F*-measures higher than or equal to 0.7. The majority of the lower value scores occur for the images with weak gradients. All these results correspond to the scenario of over-segmentation previously described where the obtained cluster containing the original upwelling area explodes offshore, mainly in the North region due to weak transaction of thermal boundaries. Fig. 4 (left column) illustrates the segmentation results obtained by the self-tuning SEC algorithm for the SST images presented in Fig. 1.

In order to compare the relative performances of the two unsupervised thresholding versions of SEC algorithm (Otsu-SEC and SelfT-SEC), against the supervised tuning thresholding (S-SEC), Table 4 summarizes the *F*-measures obtained for the three subsets of images. In each row the higher *F*-value between Otsu's and self-tuning versions of the SEC algorithm is marked in boldface. The Otsu-SEC wins in 57% of the cases while the self-tuning version wins in 43% of images. The best results mainly occur for the images with good gradients but also some noisy images present good results.

The three versions of the algorithm are implemented in MatLab R2013a. The experiments have been run on a computer with a 2.67 GHz Intel(R) core(TM) i5 processor and 6 Gbytes of RAM. The operating system is Windows 8.1 Pro, 64-bit. The elapsed time of segmenting an SST image with each of the supervised version and Otsu's thresholding version of our algorithm is 25 s. The self-

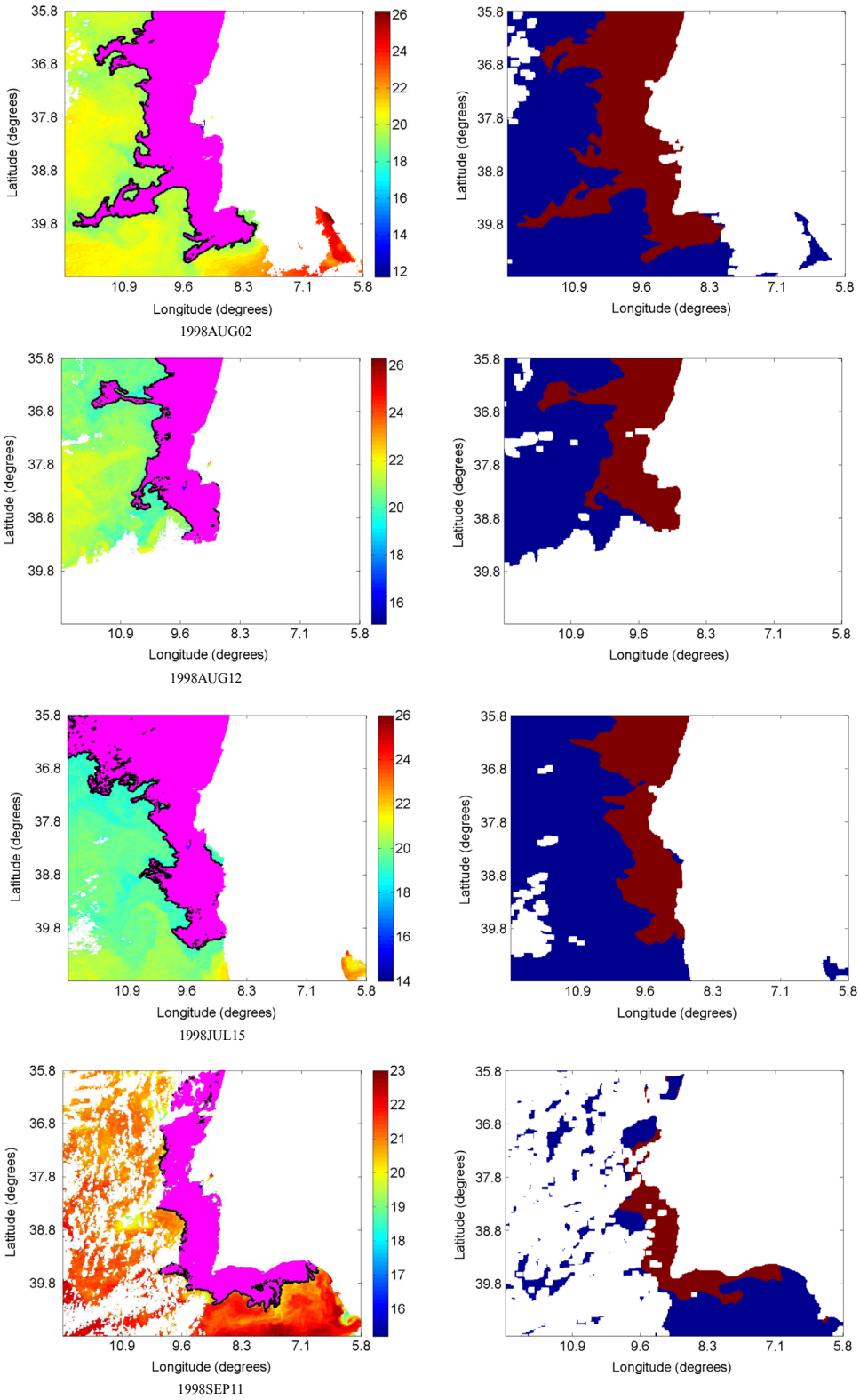

Fig. 4. Upwelling area retrieved by the self-tuning version of SEC algorithm applied to SST images of Portugal (left column) and binary ground-truth maps of the images (right column).

tuning version of SEC algorithm takes 22 s to segment one SST image.

5. Conclusion and future work

We have proposed a new method, one seed expanding cluster (SEC), inspired by the SRG approach, for the automatic segmentation of coastal upwelling from SST images. New contributions of this algorithm are: a novel homogeneity criterion (6), no order dependence of the pixel testing to be labeled, and a self-tuning version of the algorithm with the threshold derived from the approximation criterion.

Table 4
F-measures for the three versions of the SEC algorithm: supervised version of tuning parameter (S-SEC), Otsu's thresholding (Otsu-SEC), and self-tuning version (SelfT-SEC), when applied to the SST images of Portugal. In each row the higher *F*-value between Otsu's and self-tuning versions of the algorithm is marked in boldface.

SST image	S-SEC	Otsu-SEC	SelfT-SEC
Good			
1998-08-01	0.984	0.816	**0.974**
1998-08-02	0.977	0.932	**0.956**
1998-07-18	0.978	0.663	**0.955**
1998-08-12	0.973	0.899	**0.942**
1998-08-30	0.940	0.907	**0.935**
1998-08-19	0.939	**0.936**	0.898
1998-07-28	0.981	**0.977**	0.896
1998-07-24	0.942	0.870	**0.893**
1998-09-15	0.912	**0.909**	0.891
1998-07-21	0.897	0.821	**0.885**
1998-08-05	0.915	**0.921**	0.862
1998-06-28	0.968	**0.921**	0.793
1998-07-03	0.944	**0.835**	0.790
1998-08-21	0.971	**0.896**	0.717
1998-09-05	0.910	**0.715**	0.713
Weak grad.			
1998-06-23	0.951	0.753	**0.788**
1998-07-15	0.879	**0.853**	0.781
1998-08-23	0.841	**0.835**	0.729
1998-09-08	0.976	**0.827**	0.695
1998-06-25	0.969	**0.703**	0.682
1998-06-14	0.961	0.569	**0.647**
1998-07-11	0.972	**0.864**	0.627
1998-06-18	0.893	**0.900**	0.590
1998-09-24	0.642	**0.492**	**0.490**
Noisy			
1998-09-11	0.910	0.835	**0.838**
1998-09-30	0.834	0.819	**0.824**
1998-07-07	0.768	0.524	**0.689**
1998-08-10	0.670	**0.669**	0.584

The supervised and Otsu's unsupervised version of the algorithm both present very high *F*-measure on segmenting SST images showing different upwelling situations. The self-tuning version of the algorithm succeeds for all images presenting contrasting gradients between the coastal cold waters and the warming offshore waters of the upwelling region, and in some images with weak gradients for upwelling.

Further research should be directed toward the improvement of the SEC algorithm and include the following:

(i) A sequentially extracting cluster version of the algorithm to produce multi-clusters to segment the images with several discontinuous areas of upwelling.
(ii) An extensive study to compare various automatic thresholding methods, both those introduced by us and those available in the literature. Several preliminary experiments have been conducted using the Kittler and Illingworth (1986) method and the entropy-based method of Kapur and co-authors (Sezgin and Sankur, 2004) which typically lead to over-segmented results.
(iii) A study of the problem of 'explosion' presented in the segmentation of SST images with weak gradients. An explosion-controlled strategy of cluster growing has to be investigated for the self-tuning version of the algorithm to determine the optimal threshold values.

Acknowledgments

The authors thank the colleagues of Centro de Oceanografia and Department de Engenharia Geográfica, Geofísica e Energia (DEGGE), Faculdade de Ciências, Universidade de Lisboa for providing the SST images examined in this study. The authors are thankful to the anonymous reviewers for their insightful and constructive comments that allowed us to improve our paper.

Appendix A. Appendix

The Otsu's (1979) method is a nonparametric and unsupervised method for automatic threshold selection in image segmentation, taking particular importance in bimodal histograms. The method is based on dichotomizing the pixels of the image, transforming the original image into a binary one. The optimal threshold t^* is calculated starting from the calculation of the probabilities of temperature pixels. Then it is calculated as a discriminant criterion, that is, a measure of class separability, consisting on finding the feature value (in our case the temperature), t^*, for which a discriminant function, $\eta(t)$ such as the between class variance, is maximized. This corresponds to maximize the separability of the resultant classes in a binary image.

More formally, let N be the number of distinct temperature values of an image I. Let n be the total number of pixels of the image, and n_i be the number of pixels with temperature value i. Then, the probability of occurrence of the temperature i is given by $p_i = n_i/n$. The average temperature of the entire image is then

$$\mu_T = \sum_{i=1}^{N-1} i p_i \tag{16}$$

Let $C_1 = \{0, 1, \ldots, t\}$ and $C_2 = \{t+1, \ldots, L-1\}$ be the two classes corresponding to the lower temperature pixels (i.e. the pixels of interest and the background respectively) and t being the threshold value. Their respective probabilities are thus

$$\omega_1(t) = \sum_{i=1}^{t} p_i, \quad \omega_2(t) = \sum_{i=t+1}^{N-1} p_i \tag{17}$$

and their means are thus defined as

$$\mu_1(t) = \sum_{i=1}^{t} i p_i/\omega_1(t), \quad \mu_2(t) = \sum_{i=t+1}^{N-1} i p_i/\omega_2(t). \tag{18}$$

Then, the between-class variance is given by

$$\sigma_B^2(t) = \omega_1(t)(\mu_1(t) - \mu_T)^2 + \omega_2(t)(\mu_2(t) - \mu_T)^2. \tag{19}$$

The automatic optimal threshold t^* is calculated as the maximization of the between-class variance:

$$t^* = \underset{0<t<L}{\operatorname{argmax}}\{\sigma_B^2(t)\} \tag{20}$$

References

Adams, R., Bischof, L., 1994. Seeded region growing. IEEE Trans. Pattern Anal. Mach. Intell. 16, 641–647.
Arriaza, J., Rojas, F., Lopez, M., Canton, M., 2003. Competitive neural-net-based system for the automatic detection of oceanic mesoscalar structures on AVHRR scenes. IEEE Trans. Geosci. Remote Sens. 41 (4), 845–885.
Byun, Y., Kim, D., Lee, J., Kim, Y., 2011. A framework for the segmentation of high-resolution satellite imagery using modified seeded-region growing and region merging. Int. J. Remote Sens. 32 (16), 4589–4609.
Chaudhari, S., Balasubramanian, R., Gangopadhyay, A., 2008. Upwelling detection in AVHRR sea surface temperature (SST) images using neural-network framework. In: 2008 IEEE International Geoscience Remote Sensing Symposium, vol. II, pp. 926–929.
Fan, J., Yau, D.K.Y., Elmagarmid, A.K., Aref, W.G., 2001. Automatic image segmentation by integrating color-based extraction and seeded region growing. IEEE Trans. Image Process. 10 (10), 1454–1466.
Fan, J., Zeng, G., Body, M., Hacid, M.-S., 2005. Seeded region growing: an extensive and comparative study. Pattern Recognit. Lett. 26 (8), 1139–1156.

Freixenet, J., Muñoz, X., Raba, D., Martí, J., Cufí, X., 2002. Yet another survey on image segmentation: region and boundary information integration. In: Heyden, A., et al. (Eds.), Proceedings of the 7th European Conference on Computer Vision—Part III, ECCV'02. Lecture Notes in Computer Science, vol. 2352; 2002, pp. 408–452.

Grinias, I., Tziritas, G., 2001. A semi-automatic seeded region growing algorithm for video object localization and tracking. Signal Process.: Image Commun. 16 (10), 977–986.

Harikrishna-Rai, G.N., Gopalakrishnan-Nair, T.R., 2010. Gradient based seeded region grow method for CT angiographic image segmentation. Int. J. Comput. Sci. Netw. 1 (1), 1–6.

Hou, Z., Hu, Q., Nowinski, W.L., 2006. On minimum variance thresholding. Pattern Recognit. Lett. 27 (14), 1732–1743.

Ibrahim, S., Khalid, N.A., Manaf, M., 2010. Seed-based region growing (SBRG) vs adaptive network-based inference system (ANFIS) vs fuzzy *c*-means (FCM): brain abnormalities. Segmentation. Int. J. Electr. Comput. Eng. 5 (2), 94–102.

Kittler, J., Illingworth, J., 1986. Minimum error thresholding. Pattern Recognit. 19 (1), 41–47.

Kriebel, S.T., Brauer, W., Eifler, W., 1998. Coastal upwelling prediction with a mixture of neural networks. IEEE Trans. Geosci. Remote Sens. 36 (5), 1508–1518.

Mancas, M., Gosselin, B., Macq, B., 2005. Segmentation using a region growing thresholding. In: Proceedings of the SPIE, Image Processing: Algorithms and Systems IV, vol. 5672, p. 388.

Marcello, J., Marques, F., Eugenio, F., 2005. Automatic tool for the precise detection of upwelling and filaments in remote sensing imagery. IEEE Trans. Geosci. Remote Sens. 43 (7), 1605–1616.

Mat-Isa, N.A., Mashor, M.Y., Othman, N.H., 2005. Seeded region growing features extraction algorithm; its potential use in improving screening for cervical cancer. Int. J. Comput. Internet Manag. 13 (1), 61–70.

Mehnert, A., Jackway, P., 1997. An improved seeded region growing algorithm. Pattern Recognit. Lett. 18 (10), 1065–1071.

Mirkin, B., 1996. Mathematical Classification and Clustering. Kluwer, Dordrecht, The Netherlands, p. 428.

Mirkin, B., 2013. Individual approximate clusters: methods, properties, applications. In: Rough Sets, Fuzzy Sets, Data Mining, and Granular Computing. Lecture Notes in Artificial Intelligence, vol. 8170. Springer, Heidelberg, pp. 26–37.

Muñoz, X., Freixenet, J., Cufí, X., Martí, J., 2003. Strategies for image segmentation combining region and boundary information. Pattern Recognit. Lett. 24 (1–3), 375–392.

Nascimento, S., Franco, P., 2009. Segmentation of upwelling regions in sea surface temperature images via unsupervised fuzzy clustering. In: Corchado, E., Yin, H. (Eds.), Proceedings of the Intelligent Data Engineering and Automated Learning (IDEAL 2009). Lecture Notes in Computer Science, vol. 5788. Springer-Verlag, Heidelberg, Germany pp. 543–553.

Nascimento, S., Franco, P., Sousa, F., Dias, J., Neves, F., 2012. Automated computational delimitation of SST upwelling areas using fuzzy clustering. Comput. Geosci. 43, 207–216.

Nieto, K., Demarcq, H., McClatchie, S., 2012. Mesoscale frontal structures in the canary upwelling system: new front and filament detection algorithms applied to spatial and temporal patterns. Remote Sens. Environ. 123, 339–346.

Otsu, N., 1979. A threshold selection method from gray-level histograms. IEEE Trans. Syst. Man Cybern. SMC-9 (1), 62–66.

Pal, N.R., Pal, S.K., 1993. A review of image segmentation techniques. Pattern Recognit. 26 (9), 1277–1294.

Sezgin, M., Sankur, B., 2004. Survey over image thresholding techniques and quantitative performance evaluation. J. Electron. Imaging 13 (1), 146–168.

Shih, F., Cheng, S., 2005. Automatic seeded region growing for color image segmentation. Image Vis. Comput. 23, 877–886.

Ugarriza, L.G., Saber, E., Vantaram, S.R., Amuso, V., Shaw, M., Bhaskar, R., 2009. Automatic image segmentation by dynamic region growth and multiresolution merging. IEEE Trans. Image Process. 18 (10), 2275–2288.

Van Rijsbergen, C.J., 1979. Information Retrieval, 2nd ed. Butterworths, London, p. 208.

Verma, O., Hanmandlu, M., Seba, S., Kulkarni, M., Jain, P., 2011. A simple single seeded region growing algorithm for color image segmentation using adaptive thresholding. In: Proceedings of the 2011 International Conference on Communication Systems and Network Technologies. IEEE Computer Society, Washington, DC, USA, pp. 500–503.

Wang, Z., Jensen, J.R., Im, J., 2010. An automatic region-based image segmentation algorithm for remote sensing applications. Environ. Model. Softw. 25 (10), 1149–1165.

Whitney, B.W., Backman, N.J., Furst, J.D., Raicu, D.S., 2006. Single click volumetric segmentation of abdominal organs in Computed Tomography images. In: Proceedings of SPIE Medical Imaging Conference: Image Processing, p. 614-44G.

Wu, J., Poehlman, S., Noseworthy, M.D., Kamath, M., 2009. Texture feature based automated seeded region growing in abdominal MRI segmentation. J. Biomed. Sci. Eng. 2, 1–8.

Zanaty, E.A., 2013. Improved region growing method for magnetic resonance images (MRIs) segmentation. Am. J. Remote Sens. 1 (2), 53–60.

Zhang, H., Fritts, J., Goldman, S., 2008. Image segmentation evaluation: a survey of unsupervised methods. Comput. Vis. Image Underst. 110 (2), 260–280.

Zhang, T., Yang, X., Hu, S., Su, F., 2013. Extraction of coastline in aquaculture coast from multispectral remote sensing images: object-based region growing integrating edge detection. Remote Sens. 5 (9), 4470–4487.

Zhou, Y., Starkey, J., Mansinha, L., 2004. Segmentation of petrographic images by integrating edge detection and region growing. Comput. Geosci. 30, 817–831.